NASA Technical Memorandum 106302

# Buckling Analysis of Laminated Thin Shells in a Hot Environment

Pascal K. Gotsis and James D. Guptil
*Lewis Research Center*
*Cleveland, Ohio*

September 1993



NASA

# BUCKLING ANALYSIS OF LAMINATED THIN SHELLS IN A HOT ENVIRONMENT

Pascal K. Gotsis and James D. Guptil

National Aeronautics and Space Administration

Lewis Research Center

Cleveland, Ohio

CONTENTS

## SUMMARY

Results are presented of parametric studies to assess the effects of various parameters on the buckling behavior of angle-ply, laminated thin shells in a hot environment. These results were obtained by using a three-dimensional finite element analysis. An angle-ply, laminated thin shell with fiber orientation of $[\theta/\text{-}\theta]_2$ was subjected to compressive mechanical loads. The laminated thin shell had a cylindrical geometry. The laminate contained T300 graphite fibers embedded in an intermediate-modulus, high-strength (IMHS) matrix. The fiber volume fraction was 55 percent and the moisture content was 2 percent. The residual stresses induced into the laminate structure during the curing were taken into account. Parametric studies were performed to examine the effect on the critical buckling load of the following parameters: cylinder length and thickness, internal hydrostatic pressure, different ply thicknesses, different temperature profiles through the thickness of the structure, and different layup configurations and fiber volume fractions. In conjunction with these parameters the ply orientation varied from 0° to 90°. Seven ply angles were examined: 0°, 15°, 30°, 45°, 60°, 75°, and 90°.

The results show that the ply angle $\theta$ and the laminate thickness had significant effects on the critical buckling load. The fiber volume fraction, the fiber orientations, and the internal hydrostatic pressure had important effects on the critical buckling load. The cylinder length had a moderate influence on the buckling load. The thin shell with $[\theta/\text{-}\theta]_2$ or $[\theta/\text{-}\theta]_s$ angle-py laminate had better buckling-load performance than the thin shell with $[\theta]_4$ angle-ply laminate. The temperature profiles through the laminate thickness and various laminates with the different ply thicknesses had insignificant effects on the buckling behavior of the thin shells.


## INTRODUCTION

High-speed aircraft, which will operate under hostile environments at speeds that are multiples of the speed of sound, require new materials and updated numerical design approaches. New high-strength, lightweight, elevated-temperature composites that can be tailored for the required performance are

already finding applications and acceptance in aircraft frame and engine structures. Designing with these materials requires new ideas and poses challenges in materials selection, fabrication, durability, and failure mechanisms. The influence of hostile environments, nonlinear material and structural behavior, and the coupling between responses induced by various loads require complex analysis methods.

A stand-alone multidisciplinary computer code, CSTEM (Coupled Structural/Thermal/Electro-Magnetic Analysis/Tailoring) [1-4], was developed by integrating the three-dimensional finite element analysis method with several single-discipline codes including those for integrated composite mechanics [5,6].

This paper demonstrates that the CSTEM code can computationally simulate aircraft engine composite structures under compressive mechanical loads at elevated temperatures. The structure studied was a thin, cylindrical laminated shell. The angle-ply $[\theta/\text{-}\theta]_2$ laminate contained plies with uniform thickness. The residual stresses induced into the laminated composite during the curing were taken into account. Parametric studies were performed to examine the effects on the critical buckling load of parameters such as the ply angle $\theta$, the cylinder length and thickness, the laminate thickness, the internal hydrostatic pressure, the temperature profile through the thickness of the structure, different layup configurations, and the fiber volume fraction.

## BRIEF DESCRIPTION OF SIMULATION PROCEDURE

The general-purpose computer program CSTEM computationally simulates the coupled multi-disciplinary structural, heat transfer, vibration, acoustic, and electromagnetic behavior of elevated-temperature, layered, multimaterial composite structures in aggressive environments. All the disciplines are coupled for nonlinear geometrical, material, loading, and environmental effects. CSTEM is based on a modular structure as shown in Fig. 1 and is accessed by the user through its executive module. The structural response can be predicted at all the composite scales including constituents (fiber and matrix) and ply level. The composite mechanics is simulated with the ICAN (Integrated Composite Analyzer)

module [5,6], which was developed at NASA Lewis Research Center and performs, among others, through-the-thickness point stress analysis. The micromechanics equations embedded in ICAN include the effects of temperature and moisture. ICAN simulates the behavior of the polymer composites from the constituent material level to the laminate level and is depicted in Figs. 2 and 3. ICAN includes a resident material property data bank for aerospace fiber and matrix materials at room temperature. The user needs to specify only a code name for the desired material (rather than having to manually input all the properties) in the CSTEM input.

The procedure for computationally simulating composite structures is shown in Fig. 2 and consists of four parts: the constituents, the synthesis, the finite element analysis, and the decomposition. For detailed and comprehensive understanding of the computational simulation see Refs. 5 and 6. Briefly, the computational procedure is as follows:

(1) The constituents. The material properties of the fibers and the matrix, in any operational temperature and moisture conditions, are updated by using the constitutive equation depicted in Fig. 3.

(2) The synthesis.

(a) The mechanical properties of the plies are calculated from the mechanical properties of the fibers and the matrix by using micromechanics theory. Also the stiffness matrix of the stress-strain relation for each ply is computed.

(b) The extensional stiffness matrix **A**, the coupling stiffness matrix **B**, and the bending stiffness matrix **D** are computed by using classical laminate theory.

(c) The effective laminate composite engineering properties are computed [8].

(3) The finite element analysis. The finite element analysis is performed on the composite structure at the laminate scale and, among others, the resulting forces and moments are computed at each node of the finite element mesh.

Because ICAN performs through-the-thickness point stress analysis, steps (1) and (2) and the following step (4) are referred to each individual node of the finite element mesh.

(4) The decomposition.

(a) The stresses and strains in each ply are computed by using laminate theory.

(b) The stresses and strains in the matrix and the fibers for each ply are computed by using micromechanics theory.

The CSTEM code consists of approximately 76 000 FORTRAN statements and is installed on the NASA Lewis Cray YMP computer system.

## GEOMETRY, LOAD HISTORY, AND FINITE ELEMENT MODEL OF LAMINATED THIN SHELLS

The laminated thin shell had a cylindrical geometry with the following dimensions: The ratio of the longitudinal length $L$ to the inner radius $R$ was $L/R = 4$. The ratio of the inner radius $R$ to the thickness $t$ of the shell was $R/t = 33.3$. The radius $R$ was 25.4 cm. The boundary conditions were that one end was fixed and the other free (Fig. 4).

The laminate consisted of continuous fibers made of the graphite material T300 (Table 1) embedded in an intermediate-modulus, high-strength (IMHS) matrix (Table 2). The material properties of the fiber and the matrix were taken from the data bank available in CSTEM. The fiber volume fraction was 55 percent and the moisture content was 2 percent. The balanced laminate had the fiber orientations $[\theta/\text{-}\theta]_2$ and plies of equal thicknesses.

The load history of the laminated shell (Fig. 5) consisted of two parts:

(1) Thermal load. The processing of the laminated shell started at the glass transition temperature $T_g$ of the matrix (215.5 °C, table 2). The temperature was reduced to the operating temperature $T_g/2$. At the end of the processing residual stresses were induced in the laminated composite. Note that CSTEM cannot simulate the curing by reducing the glass transition temperature to the room temperature and then increasing it to the operating temperature.

(2) At the operating temperature $T_g/2$ a compressive axial load $S$ was applied at the free end of the laminated shell. The load was increased until the structures started to buckle.

The finite element mesh consisted of 760 nodes and 360 elements (Fig. 6). Each element is a three-dimensional isoparametric parallelepiped with eight nodes.

The outcome of the computational simulation of the laminated shell is discussed next.

## RESULTS AND DISCUSSION

In this section the different angle-ply, laminated cylinders with layups $[\theta/\text{-}\theta]_2$ are described and the results are presented and discussed. The parameters investigated included

(1) The effect of cylinder axial length

(2) The effect of laminate thickness

(3) The effect of different ply thicknesses

(4) The effect of internal hydrostatic pressure

(5) The effect of temperature profile

(6) The effect of layup configuration

(7) The effect of fiber volume fraction

In conjunction with cases (1) to (6) the ply angle $\theta$ was varied from 0° to 90°. Seven ply angles were examined: 0°, 15°, 30°, 45°, 60°, 75°, and 90°.

### Effects of Cylinder Length

The influence of the cylinder length in conjunction with the ply angle $\theta$ was examined to study the buckling behavior of the laminated shell. Three different length ratios $L/R$ of 2, 4, and 6 were examined. The critical buckling load is plotted for the different $\theta$ and $L/R$ in Fig. 7. The computed values of the buckling load were normalized with respect the maximum load of $1.71\times10^5$ N. The following conclusions were reached:

(1) For all $L/R$ the buckling load increased for $0° \leq \theta \leq 30°$ and decreased for $30° \leq \theta \leq 90°$. The maximum buckling load occurred at $\theta = 30°$ and the minimum occurred at $\theta = 90°$.

(2) The long cylinder ($L/R = 6$) buckled at the lowest load, and the short cylinder ($L/R = 2$) buckled at the highest load.

(3) The percent difference in the buckling load between the short and long cylinders is plotted for the different ply angles in Fig. 8. The maximum difference in buckling load between the short and long cylinders was 29.8 percent at 75°, and the minimum difference was 4.7 percent at 30°.

Thus, laminated cylinders with different $L/R$ had a maximum buckling load in the $[30/\text{-}30]_2$ layup configuration. Long cylinders had poorer buckling behavior than short cylinders in the $[75/\text{-}75]_2$ layup configuration.

## Effects of Laminate Thickness

The influence of the laminate thickness in conjunction with the ply angle $\theta$ was examined to study the buckling behavior of the laminated shell. Thin and thick cylinders were considered with thickness ratios $R/t$ of 20, 33.3, and 100. The applied thermomechanical load is shown in Fig. 5. The critical buckling load is plotted for the different $\theta$ and $R/t$ in Fig. 9. The computed values of the buckling load were normalized with respect to the maximum load of $2.73 \times 10^5$ N. The following conclusions were reached:

(1) For all $R/t$ the buckling load increased for $0 \leq \theta \leq 30°$ and decreased for $30° \leq \theta \leq 90°$. The maximum buckling load occurred at $\theta = 30°$ and the minimum occurred at $\theta = 90°$.

(2) The thin cylinder ($R/t = 100$) buckled at the lowest load, and the thick cylinder ($R/t = 20$) buckled at the highest load.

(3) The percent difference in the buckling load between the thick and the thin cylinders is plotted for the different ply angles in Fig. 8. The maximum difference in buckling load was 85.07 percent at $\theta = 30°$, and the minimum difference was 82.98 percent at at $\theta = 45°$.

Therefore, thin or thick cylinders with a $[30/-30]_2$ layup configuration maximized the buckling load. The buckling behavior of the thick cylinders was superior to that of the thin cylinders.

## Effects of Ply Thickness

The effects of laminates with various ply thicknesses in conjunction with the ply angle $\theta$ were examined to study the buckling behavior of the composite cylinder. Three laminates with different ply thicknesses were examined

(1) A $[\theta/-\theta]$ angle-ply laminate with equal ply thicknesses $(t/2,\ t/2)$

(2) A $[\theta/-\theta]_2$ angle-ply laminate with nonuniform ply thicknesses $(3t/8,\ t/8,\ t/8,\ 3t/8)$.

(3) A $[\theta/-\theta]_2$ angle-ply laminate with equal ply thicknesses $(t/4,\ t/4,\ t/4,\ t/4)$.

In all three cases the thickness ratio $R/t$ was 33.3. The critical buckling load is plotted for different $\theta$ and $t$ in Fig. 10. The computed buckling loads were normalized with respect to the maximum load of $1.45\times10^5$ N. The following conclusions were reached:

(1) The buckling load increased for $0° \leq \theta \leq 30°$ and decreased for $30° \leq \theta \leq 90°$. The maximum buckling load occurred at $\theta = 30°$ and the minimum occurred at $\theta = 90°$:

(2) The composite cylinder with $(t/2,\ t/2)$ ply thicknesses buckled at the lowest load, then the cylinder with the $(3t/8,\ t/8,\ t/8,\ 3t/8)$ ply thicknesses, and finally the cylinder with the $(t/4,\ t/4,\ t/4,\ t/4)$ ply thicknesses.

(3) The percent difference in the buckling load between the two laminates with the uniform thicknesses $(t/4,\ t/4,\ t/4,\ t/4)$ and $(t/2,\ t/2)$ is plotted for the different ply angles in Fig. 8. The maximum difference in buckling load was 8.6 percent at $\theta = 15°$, and the minimum difference was 2.7 percent at $\theta = 0°$.

Therefore, laminated cylinders with uniform or nonuniform ply thicknesses have the maximum buckling load at the $[30/-30]_2$ layup configuration. The different ply thicknesses did not significantly influence the buckling behavior of the cylinders.

## Effects of Internal Hydrostatic Pressure

The influence of the internal hydrostatic pressure $P$ in conjunction with the ply angle $\theta$ was examined to study the buckling behavior of the laminated cylinder. In addition to the hydrostatic pressure $P$, the uniform temperature $T$ and the axial compressive stress $S$ were applied (Fig. 5). Three stress ratios $S/P$ of 100, 120, and 140 were examined. The results of the analysis were compared with the load case in which temperature and compressive pressure $S$ were applied (Fig. 5).

The critical buckling load is plotted for the different ply angles $\theta$, stress $S$, and ratio $S/P$ in Fig. 11. The computed values of the critical buckling load were normalized with respect to the maximum load of $1.66\times10^5$ N. The following conclusions were reached:

(1) For all load conditions the buckling load increased for $0° \leq \theta \leq 30°$ and decreased for $30° \leq \theta \leq 90°$. The maximum buckling load occurred at $\theta = 30°$, and the minimum occurred at $\theta = 90°$.

(2) The cylinders buckled at the lowest load with the axial load $S$, then the cylinder with $S/P = 140$, the cylinder with $S/P = 120$, and finally the cylinder with $S/P = 100$.

(3) The percent difference in buckling load between the cylinder with $S/P = 100$ and the cylinder with axial stress $S$ is plotted for the different ply angles in Fig. 8. The maximum difference in the buckling load was 28.06 percent at $\theta = 60°$, and the minimum difference was 11 percent at $\theta = 30°$.

Thus, the internal hydrostatic pressure $P$ had a beneficiary influence on the buckling behavior of the cylinder and maximized the buckling load. Also at the $[30/\text{-}30]_2$ layup configuration the buckling load was maximized independent of the load conditions.

## Effects of Temperature

The effects of the temperature profile through the laminate thickness in conjunction with the ply angle $\theta$ were examined to study the buckling behavior of the cylinder. Two temperature profiles were examined: The first profile was uniform and the temperature was equal to $T_g/2$, where $T_g$ is the glass transition temperature of the matrix. The second temperature profile was linear through the laminate thickness.

The temperature of the inner surface was uniform and equal to $T_g/2$, and the outer surface was at room temperature.

The critical buckling load is plotted as a function of $\theta$ and the temperature profiles in Fig. 12. The computed values of the buckling load were normalized with respect to the maximum load of $1.601 \times 10^5$ N. The following conclusions were reached:

(1) For both temperature profiles the buckling load increased for $0° \leq \theta \leq 30°$ and decreased for $30° \leq \theta \leq 90°$. The maximum value of the buckling load occurred at $\theta = 30°$, and the minimum value occurred at $\theta = 90°$.

(2) The cylinder with the uniform temperature profile buckled at a lower temperature than the cylinder with the linear temperature profile.

(3) The percent difference in buckling load between the uniform and the linear profiles is plotted for the various ply angles in Fig. 8. The maximum difference in buckling load was 7.8 percent at $\theta = 45°$, and the minimum difference was 1.6 percent at $\theta = 60°$.

Therefore, the examined temperature profiles through the thickness of the thin cylinder did not significantly affect the buckling behavior of the structure. For both temperature profiles the buckling load was optimized at the $[30/\text{-}30]_2$ layup configuration.

## Effects of Laminates With Different Layup Configurations

The effects of the laminates with different layup configurations in conjunction with the ply angle $\theta$ were examined to study the buckling behavior of the cylinder. Three angle-ply laminates were considered: a laminate with fiber orientation of $[\theta]_4$, a balanced laminate with fiber orientations of $[\theta/\text{-}\theta]_2$, and a balanced and symmetric laminate with fiber orientations of $[\theta/\text{-}\theta]_s$. The plies had equal thickness in all laminates. The thickness ratio $R/t$ was 33.3.

The buckling analyses of the balanced and symmetric laminate $[\theta/\text{-}\theta]_s$ and the balanced laminate $[\theta/\text{-}\theta]_2$ gave identical results. Thus, the following discussion focuses only on two layup configurations $[\theta]_4$ and $[\theta/\text{-}\theta]_2$.

The buckling load is plotted for the different ply angles and for the two layup configurations in Fig. 13. The computed values of the buckling load were normalized with respect to the maximum load of $1.49\times10^5$ N. The following conclusions were reached:

(1) For both angle-ply laminates $[\theta]_4$ and $[\theta/\text{-}\theta]_2$ the buckling load increased for $0° \leq \theta \leq 30°$ and decreased for $30° \leq \theta \leq 90°$. The maximum buckling load occurred at $\theta = 30°$, and the minimum occurred at $\theta = 90°$.

(2) The composite cylinder with the laminate $[\theta]_4$ buckled at a lower load than the one with laminate $[\theta/\text{-}\theta]_2$.

(3) The percent difference in buckling load between the two angle-ply laminates is plotted for the different ply angles in Fig. 8. The maximum difference in buckling load was 30.2 percent at $\theta = 30°$, and the minimum difference was 0 at $\theta = 0°$ and $90°$.

Thus, the $[\theta/\text{-}\theta]_2$ angle-ply cylinder had superior buckling behavior in comparison with the $[\theta]_4$ angle-ply cylinder. The examined angle-ply laminates had maximum buckling loads at $\theta = 30°$.

## Effects of Fiber Volume Fraction

The effects of the fiber volume fraction in conjunction with the ply angle $\theta$ were examined to study the buckling behavior of the cylinder. Three fiber volume fractions were examined: 55, 60, and 65 percent.

The critical buckling load is plotted for the different ply angles and for the various fiber volume fractions in Fig. 14. The computed values of the buckling load were normalized with respect to the maximum load of $1.77\times10^5$ N. The following conclusions were reached:

(1) For all fiber volume fractions the buckling load increased for $0° \leq \theta \leq 30°$ and decreased for $30° \leq \theta \leq 90°$. The maximum buckling load occurred at $\theta = 30°$, and the minimum occurred at $\theta = 90°$.

(2) The composite cylinder with the lowest fiber volume fraction of 55 percent buckled at the lowest load, and the cylinder with the highest fiber volume fraction of 65 percent buckled at the highest load.

(3) The percent difference in buckling load between the two laminates with fiber volume fractions of 65 and 55 percent is plotted for the various ply angles in Fig. 8. The maximum difference in buckling load was 16 percent at $\theta = 30°$, and the minimum difference was 14.6 percent at $\theta = 75°$.

These results shows that composite cylinders with various fiber volume fractions withstood the maximum buckling load at the 30° ply angle. The fiber volume fraction had an important influence on the buckling load. An increase of 10 percent in the fiber volume fraction increased the buckling load by almost 15.5 percent.

## CONCLUSIONS

A computational simulation of the buckling behavior of hot, laminated thin shells was performed by using a three-dimensional finite element analysis. The laminated shell had a cylindrical geometry and consisted of T300 graphite fibers embedded in an intermediate-modulus, high-strength (IMHS) matrix. Parametric studies on the $[\theta/\text{-}\theta]_2$ angle-ply laminate cylinder were conducted with the following results:

(1) The ply angle $\theta$ and the laminate thickness significantly influenced the buckling behavior of the structure.

(2) The fiber volume fraction, the fiber orientations, and the internal hydrostatic pressure had an important influence on the buckling behavior of the laminated cylinder.

(3) The cylinder length had a moderate influence on the buckling behavior of the structure.

(4) The thin shell with the $[\theta/\text{-}\theta]_2$ or $[\theta/\text{-}\theta]_s$ angle-ply laminate withstood higher buckling load than the shell with the $[\theta]_4$ angle-ply laminate.

(5) The temperature profiles through the laminate thickness and the various laminates with different ply thicknesses had insignificant effects on the buckling behavior of the thin cylinder.

## ACKNOWLEDGMENT

The authors would like to thank Dr. Christos C. Chamis for his helpful discussion of the present paper.

## REFERENCES

1. M. Hartle. CSTEM User's Manual. General Electric Company, Cincinnati, OH, 1990.

2. C.C. Chamis, and S.N. Singhal. Coupled Multi-Disciplinary Simulation of Composite Engine Structures in Propulsion Environments, NASA TM-105575 (1993).

3. N.S. Singhal, P.L.N. Murthy, and C.C. Chamis. Coupled Multi-Disciplinary Composites Behavior Simulation. NASA TM-106011 (1993).

4. N.S. Singhal, et al. Computational Simulation of Acoustic Fatigue for Hot Composite Structures, NASA TM-104379 (1991).

5. P.L.N. Murthy, and C.C. Chamis. Integrated Composite Analyzer (ICAN) - User's and Programmer's Manual. NASA TP-2515 (1986).

6. C.C. Chamis. Simplified Composite Micromechanics Equations for Hygral, Thermal and Mechanical Properties. NASA TM-83320 (1987).

7. J.M. Whitney, I.M. Daniel, and R.B. Pipes. Experimental Mechanics of Fiber Reinforced Composite Materials. Society for Experimental Stress Analysis (1984).

TABLE 1.—T300 GRAPHITE FIBER PROPERTIES AT ROOM TEMPERATURE

| | |
|---|---|
| Modulus in longitudinal direction, GPa | 220.7 |
| Modulus in transverse direction, GPa | 13.79 |
| In-plane Poisson's ratio | 0.20 |
| Out-of-plane Poisson's ratio | 0.25 |
| In-plane shear modulus, GPa | 8.96 |
| Out-of-plane shear modulus, GPa | 4.827 |
| Thermal expansion coefficients in longitudinal direction, $10^{-6}$ mm/(mm-°C) | 0.99 |
| Thermal expansion coefficients in transverse direction, $10^{-6}$ mm/(mm-°C) | 10.00 |
| Thermal conductivity in longitudinal direction, W/(m-K) | 83.69 |
| Thermal conductivity in transverse direction, W/(m-K) | 8.369 |
| Fiber tensile strength, GPa | 2.413 |
| Fiber compressive strength, GPa | 2.069 |

TABLE 2.—IMHS MATRIX PROPERTIES AT ROOM TEMPERATURE

| | |
|---|---|
| Modulus in longitudinal direction, GPa | 3.448 |
| Modulus in transverse direction, GPa | 3.448 |
| In-plane Poisson's ratio | 0.35 |
| Out-of-plane Poisson's ratio | 0.35 |
| Thermal expansion coefficients in longitudinal direction, $10^{-6}$ mm/(mm-°C) | 64.8 |
| Thermal expansion coefficients in transverse direction, $10^{-6}$ mm/(mm-°C) | 64.8 |
| Thermal conductivity in longitudinal direction, W/(m-K) | 2.16 |
| Thermal conductivity in transverse direction, W/(m-K) | 2.16 |
| Matrix tensile strength, MPa | 103.4 |
| Matrix compressive strength, MPa | 241.3 |
| Matrix shear strength, MPa | 89.6 |
| Void fraction | 0.225 |
| Glass transition temperature, °C | 215.55 |

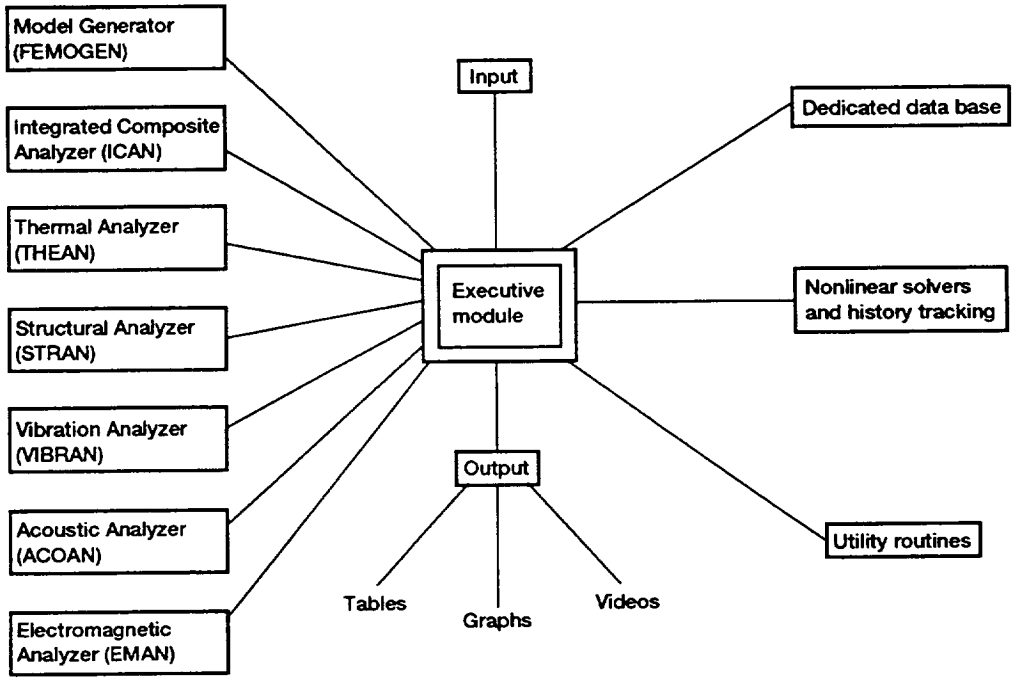


Figure 1.—CSTEM modular structure.

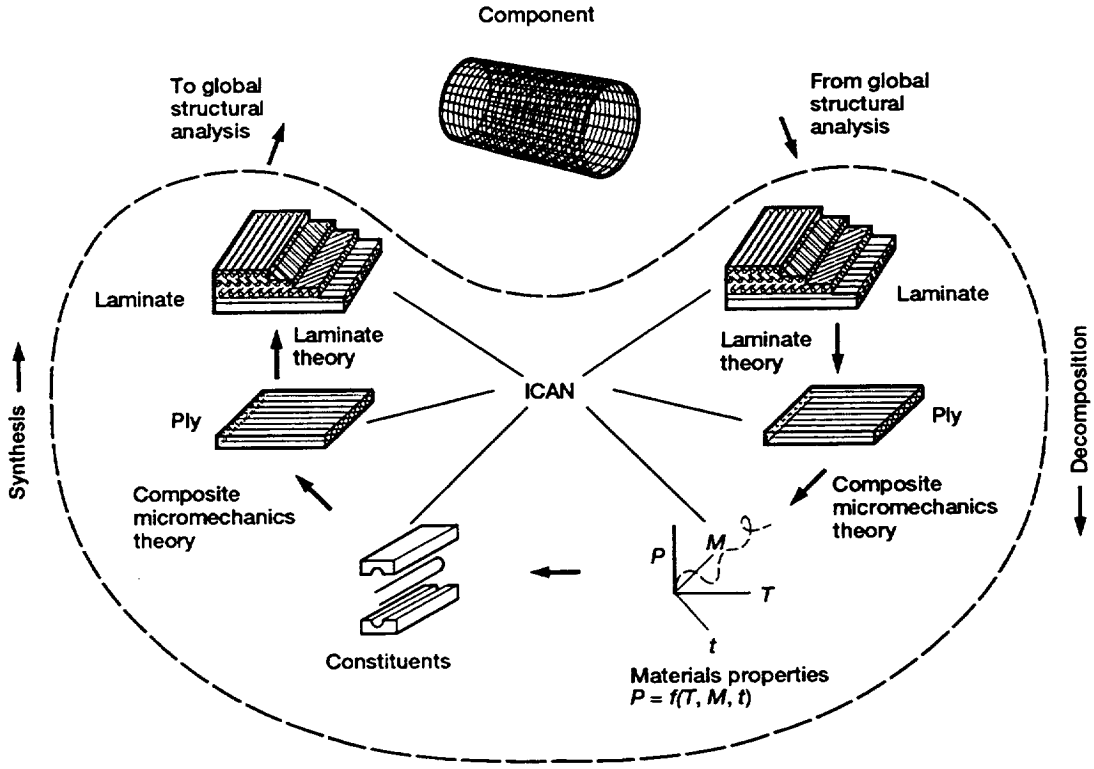


Figure 2.—Integrated Composite Analyzer (ICAN).

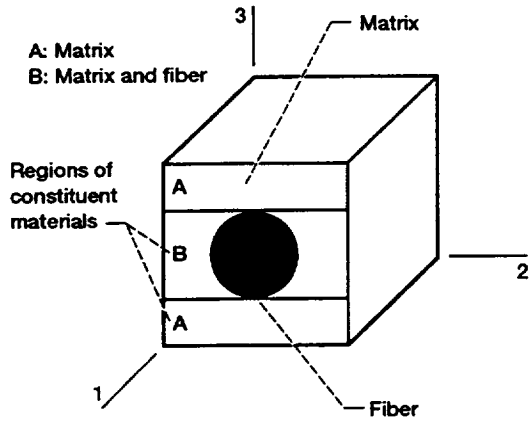


$$\frac{P_M}{P_{M0}} = \left(\frac{T_{GW} - T}{T_{GD} - T_0}\right)^{1/2}$$

$$T_{GW} = (0.005\,M^2 - 0.1M + 1)T_{GD}$$

$P_M$ matrix property at current temperature $T$
$P_{M0}$ matrix property at reference temperature $T_0$
$T_{GW}$ wet glass transition temperature
$T_{GD}$ dry glass transition temperature
$M$ moisture

Figure 3.—Regions of constituent materials and nonlinear material characterization model.

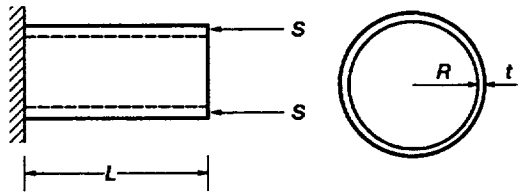


(a) Geometry: $L/R = 4$; $R/t = 33.3$; $R = 25.4$ cm.

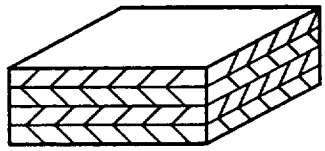

Angle-ply laminate $[\theta/\text{-}\theta]_2$

(b) Materials: fiber volume ratio = 55%; moisture = 2%; T300 fibers; IMHS matrix.

Figure 4.—Geometry and materials of laminated thin shells.

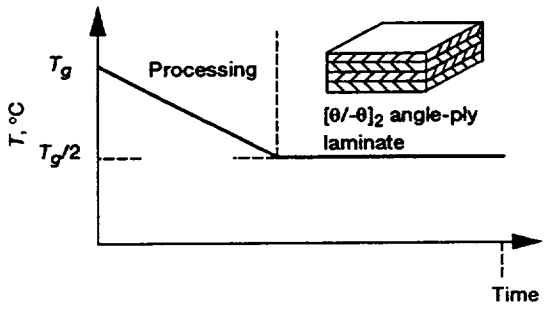


(a) Thermal load $T_g$ = 215.5 °C.

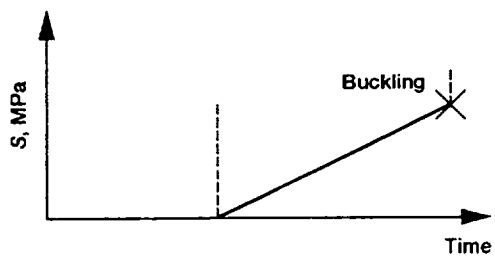


(b) Axial compressive load $S$.

Figure 5.—Load history.

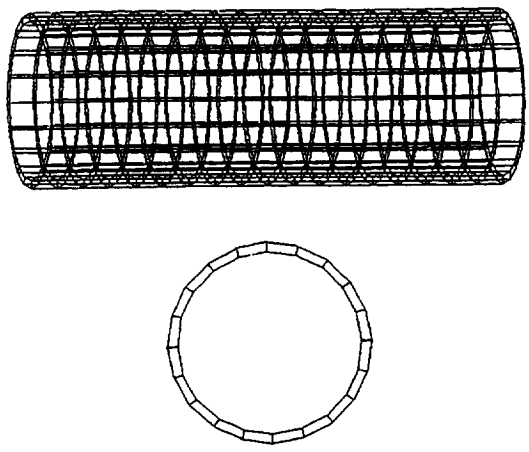

Figure 6.—Three-dimensional finite element mesh and transverse cross-sectional area of laminated thin shells.

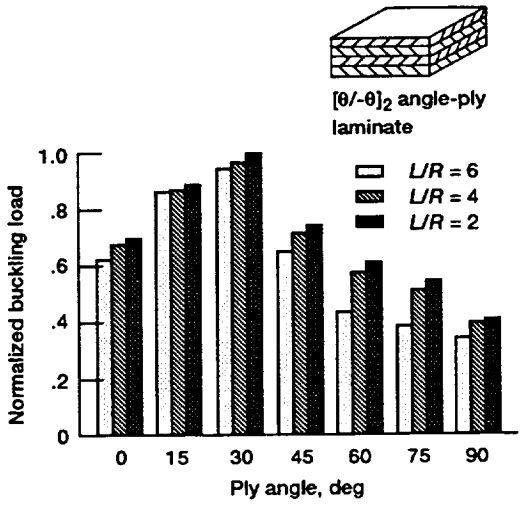


Figure 7.—Influence of length ratio $L/R$ on buckling behavior of laminated thin shells. $R/t$ = 33.3; FVR = 55%; $T = T_g/2$; moisture = 2%.

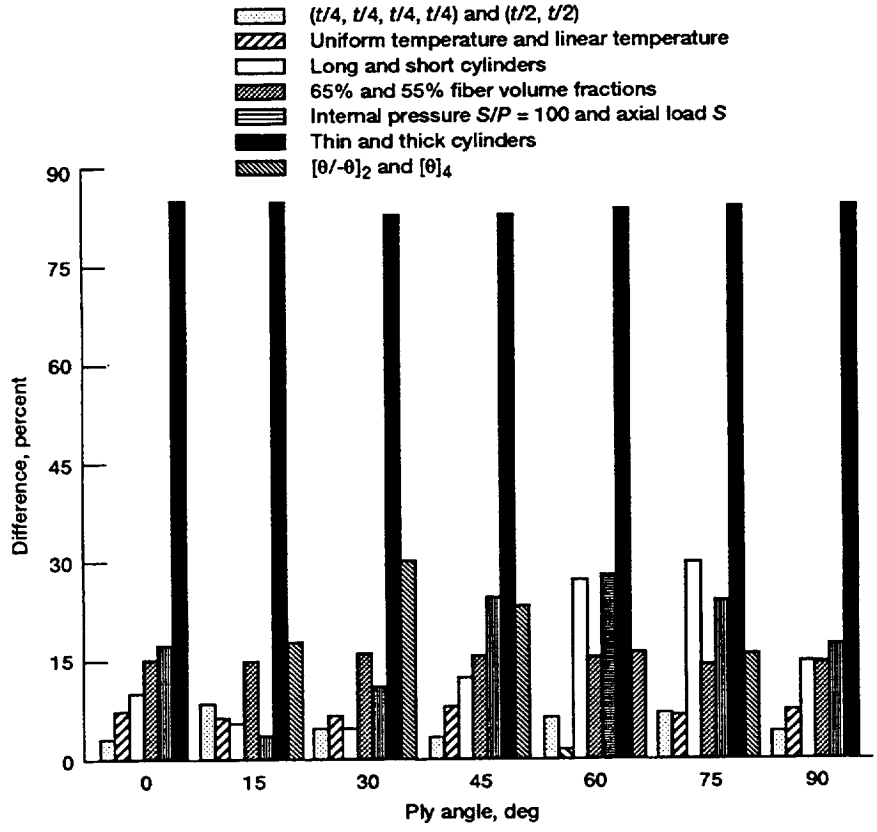


Figure 8.—Percent difference comparison of buckling load for different parameters.

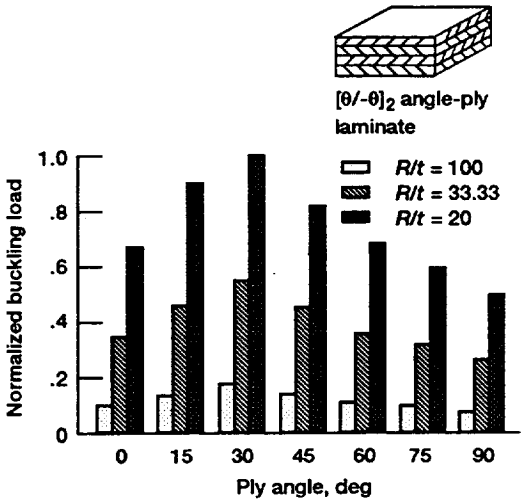


Figure 9.—Influence of thickness ratio $R/t$ on buckling behavior of laminated thin shell. $L/R$ = 4; FVR = 55%; $T = T_g/2$; moisture = 2%.

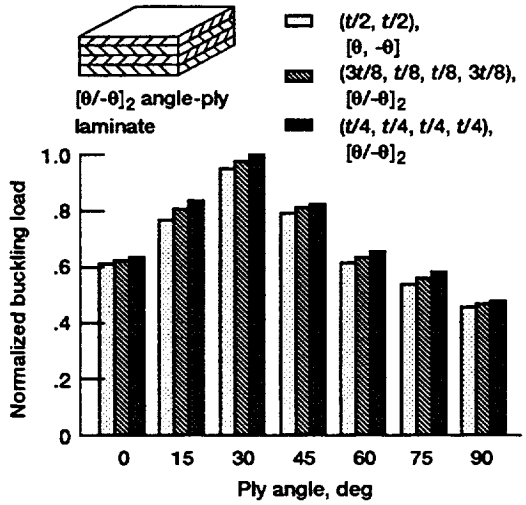


Figure 10.—Influence of ply thickness on buckling behavior of laminated thin shells. $L/R$ = 4; $R/t$ = 33.3; FVR = 55%; $T = T_g/2$; moisture = 2%.

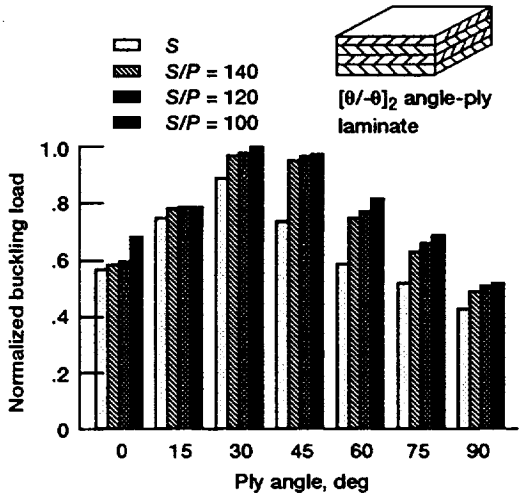


Figure 11.—Influence of internal hydrostatic pressure on buckling behavior of laminated thin shells. $L/R$ = 4; $R/t$ = 33.3; FVR = 55%; $T = T_g/2$; moisture = 2%.

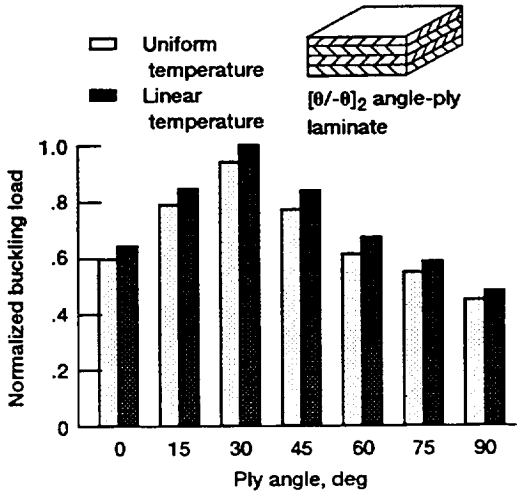


Figure 12.—Influence of temperature profile on buckling behavior of laminated thin shells. $L/R$ = 4; $R/t$ = 33.3; FVR = 55%; moisture = 2%.

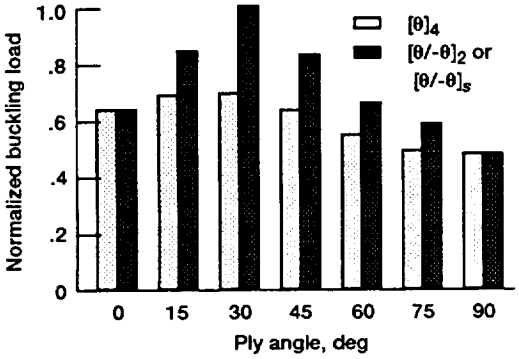


Figure 13.—Influence of layup configuration on buckling behavior of laminated thin shells. $L/R$ = 4; $R/t$ = 33.3; FVR = 55%; $T = T_g/2$; moisture = 2%.

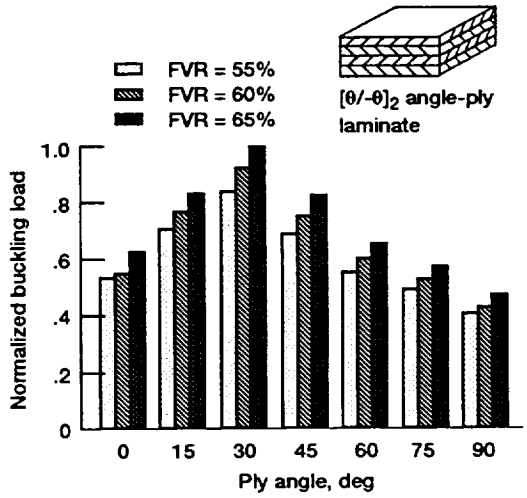


Figure 14.—Influence of fiber volume fraction (FVR) on buckling behavior of laminated thin shells. $L/R$ = 4; $R/t$ = 33.3; $T = T_g/2$; moisture = 2%.

# REPORT DOCUMENTATION PAGE

Form Approved
OMB No. 0704-0188



| 1. AGENCY USE ONLY (Leave blank) | 2. REPORT DATE | 3. REPORT TYPE AND DATES COVERED |
|---|---|---|
| | September 1993 | Technical Memorandum |

**4. TITLE AND SUBTITLE**

Buckling Analysis of Laminated Thin Shells in a Hot Environment

**5. FUNDING NUMBERS**

WU-537-04-20

**6. AUTHOR(S)**

Pascal K. Gotsis and James D. Guptil

**7. PERFORMING ORGANIZATION NAME(S) AND ADDRESS(ES)**

National Aeronautics and Space Administration
Lewis Research Center
Cleveland, Ohio 44135-3191

**8. PERFORMING ORGANIZATION REPORT NUMBER**

E-8043

**9. SPONSORING/MONITORING AGENCY NAME(S) AND ADDRESS(ES)**

National Aeronautics and Space Administration
Washington, D.C. 20546-0001

**10. SPONSORING/MONITORING AGENCY REPORT NUMBER**

NASA TM-106302

**11. SUPPLEMENTARY NOTES**

Responsible person, Pascal K. Gotsis, (216) 433-3331.

**12a. DISTRIBUTION/AVAILABILITY STATEMENT**

Unclassified - Unlimited
Subject Category 39

**12b. DISTRIBUTION CODE**

**13. ABSTRACT** *(Maximum 200 words)*

Results are presented of parametric studies to assess the effects of various parameters on the buckling behavior of angle-ply, laminated thin shells in a hot environment. These results were obtained by using a three-dimensional finite element analysis. An angle-ply, laminated thin shell with fiber orientation of $[\theta/-\theta]_2$ was subjected to compressive mechanical loads. The laminated thin shell had a cylindrical geometry. The laminate contained T300 graphite fibers embedded in an intermediate-modulus, high-strength (IMHS) matrix. The fiber volume fraction was 55 percent and the moisture content was 2 percent. The residual stresses induced into the laminate structure during the curing were taken into account. Parametric studies were performed to examine the effect on the critical buckling load of the following parameters: cylinder length and thickness, internal hydrostatic pressure, different ply thicknesses, different temperature profiles through the thickness of the structure, and different layup configurations and fiber volume fractions. In conjunction with these parameters the ply orientation was varied from 0° to 90°. Seven ply angles were examined: 0°, 15°, 30°, 45°, 60°, 75°, and 90°. The results show that the ply angle θ and the laminate thickness had significant effects on the critical buckling load. The fiber volume fraction, the fiber orientations, and the internal hydrostatic pressure had important effects on the critical buckling load. The cylinder length had a moderate influence on the buckling load. The thin shell with $[\theta/-\theta]_2$ or $[\theta/-\theta]_s$ angle-ply laminate had better buckling-load performance than the thin shell with $[\theta]_4$ angle-ply laminate. The temperature profiles through the laminate thickness and various laminates with the different ply thicknesses has insignificant effects on the buckling behavior of the thin shells.

**14. SUBJECT TERMS**

Laminated thin shells; Laminated cylinders; Angle-ply laminate; Composite structures; Computational simulation; Residual stresses; High temperature; Moisture; Structural analysis; Finite element analysis; Buckling analysis

**15. NUMBER OF PAGES**

20

**16. PRICE CODE**

A03

| 17. SECURITY CLASSIFICATION OF REPORT | 18. SECURITY CLASSIFICATION OF THIS PAGE | 19. SECURITY CLASSIFICATION OF ABSTRACT | 20. LIMITATION OF ABSTRACT |
|---|---|---|---|
| Unclassified | Unclassified | Unclassified | |